

Sojourn Time of Moving Relays in Dual-Hop Cooperative Communication

Submitted in partial fulfillment of
the requirements for the degree of

Bachelor of Technology
in Electrical Engineering
&
Master of Technology
in Communications and Signal Processing

by

Prudhvi Porandla
110070039

Under the guidance of
Prof. S. N. Merchant



Department of Electrical Engineering
Indian Institute of Technology Bombay
2016

Dissertation Approval

The dissertation entitled *Sojourn Time of Moving Relays in Dual-Hop Cooperative Communication* by *Prudhvi Porandla (110070039)* is approved for the degree of *Bachelor of Technology* in *Electrical Engineering* and *Master of Technology* in *Communications and Signal Processing*.

.....

Examiner

.....

Examiner

.....

Supervisor

.....

Chairman

Date: June 20, 2016

Place: IIT Bombay

Declaration

I declare that this written submission represents my ideas in my own words and wherever others' ideas or words have been included, I have adequately cited and referenced the original sources. I also declare that I have adhered to all principles of academic honesty and integrity and have not misrepresented or fabricated or falsified any idea/ data/ fact/ source in my submission. I understand that any violation of the above will be cause for disciplinary action by IIT Bombay and can also evoke penal action from the sources which have thus not been properly cited or from whom proper permission has not been taken when needed.

Prudhvi Porandla

Date: June 20, 2016

Place: IIT Bombay

Acknowledgements

I would to express my heartfelt gratitude to my guide Prof. S. N. Merchant for his constant encouragement and patience throughout the project. I would like to thank him for offering moral support to work on the project by placing overwhelming amount of trust in me.

I would like to thank Kesav Kaza for his support, advice and presence during every technical discussion and brainstorming session. This work is essentially the summation of all the ideas exchanged during those sessions. I would like to thank all SPANN lab members for making every moment in the lab a learning experience. Special thanks to Zoheb for providing some of the figures. Finally, my wholehearted thanks to the faculty members of Electrical Engineering Department for imparting me with invaluable knowledge.

I owe my deepest gratitude to my parents for their relentless support throughout my life and their patience during my DDP work. To the power that drives the Nature without which nothing is possible.

June 20, 2016

Prudhvi Porandla

Abstract

We explore the application of relaying in cellular networks and study various cooperation policies. We propose a cooperation policy for downlink using the same principles that were used to design policies in uplink case. We then discuss the case where relays are moving according to a random waypoint(RWP) mobility model. We attempt to find the sojourn time of a relay in the feasible region and present the challenges involved. As a first advance towards finding the sojourn time we give a general expression for the probability that a relay leaves the feasible region in one step that can be used for any mobility model. We use the probability to find the expected number of transitions a node makes before leaving the region and compare it with the simulation results. Finally we present the idea of modelling the node movement as a Markov Chain and to use the results of Absorbing Markov Chain to find the expected number of transitions more accurately.

Contents

Abstract	i
List of Figures	v
1 Introduction	1
2 Relaying and Cooperation Policies	3
2.1 Partial Decode-and-Forward Relaying	3
2.1.1 Signal Design	3
2.1.2 Channel Model	4
2.1.3 Achievable Rate	5
2.2 Cellular Network Geometry and User-Assisted Relaying	6
2.2.1 Network geometry model	6
2.2.2 Channel Model	7
2.2.3 Interference	7
2.2.4 Equivalent Standard Channel Model	8
2.3 Cooperation Policies and Probability	9
2.3.1 Policies	9
2.3.2 Cooperation Probabilities	10
2.4 Interference Analysis	13
2.4.1 First Two Moments of Interference Power	13
2.4.2 Modelling Interference Power Distribution	15
2.5 Simulations and Results	16
2.5.1 Simulation Setting	16
2.5.2 Results	17
2.6 Downlink Cooperation Policy	19

3	Moving Relays	21
3.1	Mobility Model	21
3.1.1	Rayleigh RWP Model	21
3.2	Mean Sojourn Time	23
3.3	Probability of leaving in one transition	24
3.3.1	Boundaries of the region	24
3.3.2	Probability	28
3.4	Expected number of transitions	30
4	Mobility Markov Chain	32
5	Simulations and Results	34
5.1	$E[L]$	34
5.2	$\rho(r, \theta)$	35
5.2.1	$\rho(r, \theta)$ vs. λ	35
5.2.2	$\rho(r, \theta)$ for different θ	36
5.3	$E[N]$	38
6	Conclusion and Further Work	39
6.1	Conclusion	39
6.2	Further Work	39
	Bibliography	40

List of Figures

2.1	Transmission phases in PDF relaying	4
2.2	Sample layout of a cellular network ($\lambda_2 = 2\lambda_1$)	6
2.3	Network Layout	17
2.4	Corrected cooperation probability of E_3	18
2.5	Cooperation probabilities of E_2, E_3 versus user density ratio	18
2.6	Average rate per user; $\lambda = \lambda_2/\lambda_1$	19
2.7	Distances for Downlink Cooperation	19
2.8	Feasible region	20
3.1	Sample traces of rayleigh RWP mobility model	22
3.2	Initial Position is (r, θ)	24
3.3	Initial Position is (r, θ)	25
3.4	α_1	26
3.5	Previous fig. without circles	26
3.6	α_2	27
3.7	α_2 without circles	28
5.1	Mean transition length vs. λ	35
5.2	$\rho(r, 0)$ vs. λ	36
5.3	$\rho(r, \theta)$ at different angles	37
5.4	Expected number of transitions	38

Chapter 1

Introduction

With the advances in D2D communications and relaying techniques, user-assisted relaying is a viable option to improve rate and coverage in cellular networks. There are many problems that need to be solved to do this correctly viz. providing incentives for the relaying users, power allocation at both source and relay, selecting a relay that gives better rate for maximum amount of time etc.

A relay selection policy is a set of rules, which are essentially thresholds on parameters of a relay, by which an idle user can be chosen to act as a relay. The amount of time an idle user-equipment can provide relaying service is a decision parameter along with the channel conditions which dictate the rate. With this as preface it is clear that studying mobility of relays and providing analytical results for the necessary parameters is of great importance.

In [1], Xingqin Lin et al. proposed a random waypoint(RWP) mobility model that fits better with the truncated Levy walk, which is based on real mobility traces, compared to the classical RWP model and applied it to find handover rate and sojourn time in hexagonal as well as Poisson-Voronoi tessellation network geometry. To find the analytical expression for cell sojourn time, the distribution of nodes during the first movement period is derived. If the node starts at origin and moves to X_1 during the first transition, the node distribution between O and X_1 is given by

$$f(r, \theta) = \frac{\sqrt{\lambda}}{\pi r} \exp(-\lambda \pi r^2) \quad (1.1)$$

This can be interpreted as the ratio of the fraction of transition time spent in a small region $A(r, \theta)$ around the point (r, θ) to the area of the region. This can be used to find the sojourn time in one shot by integrating the distribution over the region of interest and multiplying the result with the mean transition time. However, this method places restriction on the initial position on the node and it is challenging to find a closed form expression for sojourn time if the region of interest is not a regular/well-defined shape like a hexagon. Also, we can find the sojourn time for only one movement period, which is not the case in larger regions.

After a failed attempt to find the sojourn time of a relay using node distribution 1.1, we fallback to the basic definitions in RWP model to solve the problem.

Organization of the report

The organization of the report is as follows:

1. **Chapter 2** contains the work done during the first phase of the project on PDF relaying, cooperation policies and rate gain when relaying is employed in cellular networks.
2. **Chapter 3** In this chapter we describe the mobility model and derive an expression for the probability with which a node¹ moves out of the region in one step as a function of node's starting point.
3. **Chapter 4** presents the idea of modelling mobility as a Markov Chain and using the results of Absorbing Markov Chains to find expected number of transitions.
4. **Chapter 5** analyses the probability of leaving the region in one step at different points in the region and see how it varies with λ , the mobility parameter.
5. **Conclusion and Further Work**

¹The terms node and relay have been used interchangeably

Chapter 2

Relaying and Cooperation Policies

This chapter is heavily based on the published work [2] of Hussain Elkotby and Mai Vu of Tufts University. Analysis and simulations of their work was done during first phase of the project to gain insights into signal design of various relaying schemes and to learn about the ways in which cellular networks are modelled and analysed, what challenges user-assisted relaying presents. The only subject in this chapter that will be useful for the later part of this report is presented in section 2.6.

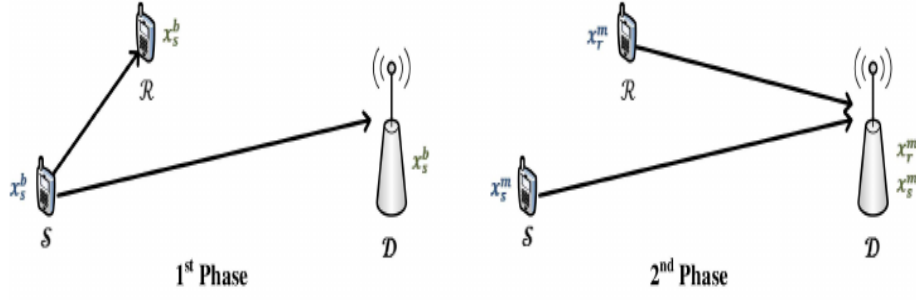
2.1 Partial Decode-and-Forward Relaying

In this section, we discuss the signal design, channel model and achievable rate of PDF relaying scheme.

2.1.1 Signal Design

Consider a source \mathcal{S} , its relay \mathcal{R} and the destination \mathcal{D} . Each transmission block is divided into two phases: 1. broadcast transmission in which \mathcal{S} broadcasts to both \mathcal{R} and \mathcal{D} . 2. multiple access transmission in which both \mathcal{S} and \mathcal{R} transmit to \mathcal{D} . In each block of transmission, \mathcal{S} splits its information into a common part and a private part. The common part is encoded via U_s^b in the 1st phase and $U_s^{m_1}$ in the 2nd phase; and the private part is encoded via $V_s^{m_2}$ in the 2nd phase. The relay \mathcal{R} decodes the information sent by \mathcal{S} in first phase and encodes the same information using $U_s^{m_1}$ in the 2nd phase.

¹Image Source: [2] Hussain Elkotby

Figure 2.1: Transmission phases in PDF relaying¹

The signals transmitted by \mathcal{R} and \mathcal{S} are as follows:

$$\text{Phase 1: } x_s^b = \sqrt{P_s^b} U_s^b, \quad (2.1)$$

$$\text{Phase 2: } x_r^m = \sqrt{P_r^m} U_s^{m_1}, \quad (2.2)$$

$$x_s^m = \sqrt{P_s^{m_1}} U_s^{m_1} + \sqrt{P_s^{m_2}} V_s^{m_2} \quad (2.3)$$

All codewords above are picked from independent Gaussian codebooks with zero mean and unit variance.

Power Constraints: Let P_s and P_r be the transmit powers of \mathcal{S} and \mathcal{R} respectively and α_1 be the fraction of transmission time allocated to first phase, then the following average power constraints should to be satisfied:

$$\alpha_1 P_s^b + \alpha_2 P_s^m = P_s, \quad \alpha_2 P_r^m = P_r \quad (2.4)$$

where $\alpha_2 = 1 - \alpha_1$

2.1.2 Channel Model

Considering the transmit signals presented above and assuming flat fading over the two phases, the received signals at \mathcal{R} and \mathcal{D} during first phase are

$$Y_r^b = h_{sr} x_s^b + Z_r^b, \quad Y_d^b = h_{sd} x_s^b + Z_d^b \quad (2.5)$$

where b denotes broadcast mode, Z_r^b and Z_d^b are *i.i.d* circularly-symmetric complex gaussians with mean 0 and variance σ^2 - $\mathcal{CN}(0, \sigma^2)$ that represent noises at \mathcal{R} and \mathcal{D} .

Similarly the received signal at \mathcal{D} during second phase can be modelled as

$$Y_d^m = h_{sd}x_s^m + h_{rd}x_r^m + Z_d^m \quad (2.6)$$

here m denotes multicast transmission; all others have usual meaning. The above expression is true only if \mathcal{D} has knowledge about the phase offset between \mathcal{S} and \mathcal{R} . This assumption is justified by noting that the phase offset between the two nodes can be estimated at base station.

2.1.3 Achievable Rate

With transmit signals in equations 2.1- 2.3 and joint ML decoding rule at \mathcal{D} , the achievable rate for this relaying scheme is:

$$R_{PDF} \leq \min(C_1 + C_2, C_3) \quad (2.7)$$

$$\text{where } C_1 = \alpha_1 \log \left(1 + |h_{sr}|^2 P_s^b \right), \quad (2.8)$$

$$C_2 = \alpha_2 \log \left(1 + |h_{sd}|^2 P_s^{m_2} \right), \quad (2.9)$$

$$C_3 = \alpha_1 \log \left(1 + |h_{sd}|^2 P_s^b \right) + \alpha_2 \log \left(1 + |h_{sd}|^2 P_s^{m_2} + \left(|h_{sd}| \sqrt{P_s^{m_1}} + |h_{rd}| \sqrt{P_r^m} \right)^2 \right) \quad (2.10)$$

C_1 represents the rate of the common part that can be decoded at \mathcal{R} , C_2 the private part that can be decoded at \mathcal{D} provided the common part has been decoded correctly, and C_3 both the common and private parts that can be jointly decoded at \mathcal{D} . These rates are achievable provided full CSI at all receivers and the source-relay phase offset knowledge.

Now that we know what PDF relaying scheme is and the achievable rate, let us see how this scheme performs in cellular networks. To analyse system performance under PDF relaying, we need to know network geometry i.e., how the users and base stations are distributed, how many users can take advantage of relaying, how users identify a potential relay etc. In the next couple of sections we describe network geometry, received signals and interference model when relaying is deployed in the whole network, and cooperation policies.

2.2 Cellular Network Geometry and User-Assisted Relaying

2.2.1 Network geometry model

Consider a cellular system which consists of multiple cells, each cell has a single base station and each base station serves multiple users. Each of the users uses a distinct frequency block. Each user is served by the single base station that is closest to that user.

We use stochastic geometry to describe the uplink cellular network. We assume that the active users in different cells that use the same resource block and cause interference to each other are distributed on a two-dimensional plane according to a homogeneous and stationary Poisson point process (PPP) Φ_1 with intensity λ_1 . The set of user equipments (UEs) that are in idle state and can participate in relaying are distributed according to another PPP Φ_2 with intensity λ_2 . We assume Φ_1 and Φ_2 are independent. Furthermore, under the assumption that each BS serves a single mobile in a given resource block, the BS should be closer to its served UE than to any other UE. Therefore we assume each BS is uniformly distributed in the Voronoi cell of its served UE. Fig. 2.2 shows an example layout of the network.

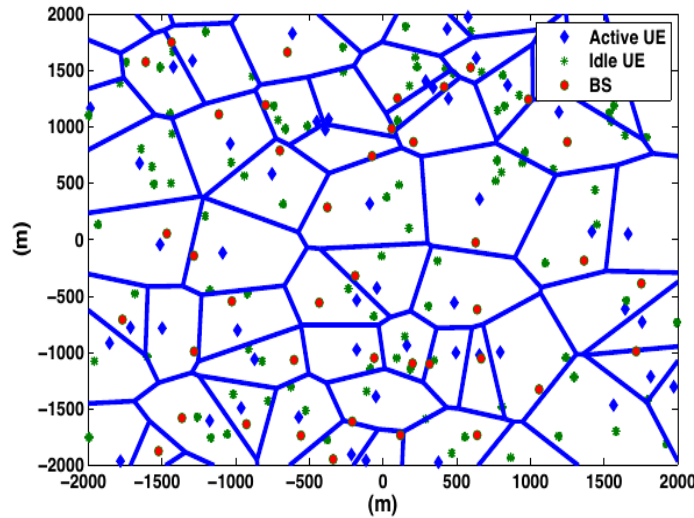


Figure 2.2: Sample layout of a cellular network ($\lambda_2 = 2\lambda_1$)²

²Image Source: [2] Hussain Elkotby

2.2.2 Channel Model

In this section, we describe the channel model when PDF relaying is deployed in cellular network. In this case, there will be out-of-cell interference in addition to noise. The interference is due to frequency reuse in other cells.

Consider i^{th} active UE, we model the received signals at the relay and base station in this cell during 1st phase as

$$\begin{aligned} Y_{r,i}^b &= h_{sr}^{(i)} x_{s,i}^b + I_{r,i}^b + Z_{r,i}^b, \\ Y_{d,i}^b &= h_{sd}^{(i)} x_{s,i}^b + I_{d,i}^b + Z_{d,i}^b \end{aligned} \quad (2.11)$$

where $I_{r,i}^b$ and $I_{d,i}^b$ represent the interference received at the i^{th} relay and destination.

In second phase of the transmission, the received signal at the BS can be modelled as

$$Y_{d,i}^m = h_{sd}^{(i)} x_{s,i}^m + h_{rd}^{(i)} x_{r,i}^m + I_{d,i}^m + Z_{d,i}^m \quad (2.12)$$

2.2.3 Interference

To model interference, we assume perfect frame synchronization. LTE-Advanced imposes very strict requirements on synchronization anyway. Interference at the relay during first phase and at the destination(BS) during first and second phases can be expressed as

$$\begin{aligned} I_{r,i}^b &= \sum_{k \neq i} B_k h_{sr}^{(k,i)} x_{s,k}^b + (1 - B_k) h_{sr}^{(k,i)} x_{s,k}, \\ I_{d,i}^b &= \sum_{k \neq i} B_k h_{sd}^{(k,i)} x_{s,k}^b + (1 - B_k) h_{sd}^{(k,i)} x_{s,k}, \\ I_{d,i}^m &= \sum_{k \neq i} B_k \left(h_{sd}^{(k,i)} x_{s,k}^m + h_{rd}^{(k,i)} x_{r,k}^m \right) + (1 - B_k) h_{sd}^{(k,i)} x_{s,k} \end{aligned} \quad (2.13)$$

the summation is over all active users. Here, $h_{sd}^{(k,i)}$ and $h_{rd}^{(k,i)}$, respectively, are the channel fading from the k^{th} active UE in Φ_1 and the associated relaying UE in Φ_2 to the BS associated with the i^{th} active UE in Φ_1 ; and $h_{sr}^{(k,i)}$ is the channel fading from the k^{th} active UE in Φ_1 to the relaying UE associated with the i^{th} active UE in Φ_1 .

B_k in above expressions is a Bernoulli random variable with success probability ρ . $B_k = 1$ is used to indicate the k^{th} active UE's decision to exploit the help of another idle UE, a relay, and apply the relaying transmission strategy, and $B_k = 0$ indicates that the k^{th} UE has no relay. In section 2.3, we derive the cooperation probability ρ for different cooperation policies.

For a given setting of nodes locations, based on the interference model in Eq. 2.13, we can use the fact that interference at either the relay or destination is the sum of an infinite number of signals undergoing independent fading from nodes distributed in the infinite 2-D plane and use the law of large numbers to approximate the interference as a complex Gaussian distribution. Also, since the transmitted codewords are complex Gaussian with zero mean, mean of interference is zero. To fully characterize interference as a complex Gaussian distribution, we define their distributions as $I_{d,i}^b \sim \mathcal{CN}(0, \mathcal{Q}_{d,i}^b)$, $I_{d,i}^m \sim \mathcal{CN}(0, \mathcal{Q}_{d,i}^m)$, and $I_{r,i}^b \sim \mathcal{CN}(0, \mathcal{Q}_{r,i})$ with the variances derived later in Section 2.4. The power of these interference terms which correspond to the variance of the Gaussian random variables are function of node locations and hence vary with different network realizations.

2.2.4 Equivalent Standard Channel Model

Using the interference model discussed above, we can convert the channel model in case of relaying into the standard form to capture the effects of interference into the channel fading as

$$\begin{aligned}\tilde{Y}_{r,i}^b &= \tilde{h}_{sr}^{(i)} x_{s,i}^b + \tilde{Z}_{r,i}^b, \\ \tilde{Y}_{d,i}^b &= \tilde{h}_{sd}^{(i)} x_{s,i}^b + \tilde{Z}_{d,i}^b, \\ \tilde{Y}_{d,i}^m &= \tilde{h}_{sd}^{(i)} x_{s,i}^m + \tilde{h}_{rd}^{(i)} x_{r,i}^m + \tilde{Z}_{d,i}^m\end{aligned}$$

where the new channel fading terms are defined as

$$\tilde{h}_{sr}^{(i)} = \frac{h_{sr}^{(i)}}{\sqrt{\mathcal{Q}_{r,i} + \sigma^2}}, \quad \tilde{h}_{sd}^{(b,i)} = \frac{h_{sd}^{(i)}}{\sqrt{\mathcal{Q}_{d,i}^b + \sigma^2}}, \quad \tilde{h}_{sd}^{(m,i)} = \frac{h_{sd}^{(i)}}{\sqrt{\mathcal{Q}_{d,i}^m + \sigma^2}}, \quad \tilde{h}_{rd}^{(i)} = \frac{h_{rd}^{(i)}}{\sqrt{\mathcal{Q}_{d,i}^m + \sigma^2}}$$

and the noise terms are now all $\mathcal{CN}(0, 1)$. Using these equivalent standard channels, we can compute the transmission rate using Eq. 2.7

2.3 Cooperation Policies and Probability

In this section, we look at three cooperation policies: an ideal policy E_1 , a pure geometric policy E_2 and a hybrid policy E_3 that defines whether an active UE should select an inactive UE to use it in PDF relaying. Also, expressions for cooperation probabilities of E_2 and E_3 are derived.

2.3.1 Policies

Ideal Policy E_1

The ideal cooperation policy E_1 requires the active UE nodes to know instantaneous SINRs of the relay link($\mathcal{S} - \mathcal{R}$) and the direct link($\mathcal{S} - \mathcal{D}$). The policy is defined as

$$E_1 = \left\{ |\tilde{h}_{(sr)}^{(k)}|^2 \geq |\tilde{h}_{(sd)}^{(k)}|^2 \right\} \\ \simeq \left\{ \frac{g_{sr}r_2^{-\alpha}}{\mathcal{Q}_{r,k}} \geq \frac{g_{sd}r_1^{-\alpha}}{\mathcal{Q}_{d,k}^b} \right\}$$

where r_1 and r_2 denote the direct distance between \mathcal{S} and \mathcal{D} and cooperation distance between \mathcal{S} and its closest idle UE, respectively and α is pathloss exponent. This event E_1 identifies whether an idle UE will be associated as a relay for the k^{th} UE and participate in transmission. Noise variance σ^2 is ignored since interference power dominates.

Since interference at relay and destination during first phase is more or less the same and g_{sr}, g_{sd} are identically distributed, we can safely ignore them and propose a policy that depends only on distances.

Pure Geometric Policy E_2

This policy is defined as

$$E_2 = \{r_2 \leq r_1, D \leq r_1\} \tag{2.14}$$

where D is the distance between \mathcal{R} and \mathcal{D} . In words, if source's(active UE's) nearest idle neighbour is in the intersection region of two circles of radius r_1 centered at source and destination, then that idle UE will be chosen to act as a relay.

E_2 is more practical than policy E_1 in the sense that it does not require full knowledge of both the channel fading and the interference at the decision making node. Instead, it only requires the decision making nodes to know the distances from the active user to the nearest idle user and to the base station. It represents a practical decision making strategy for fast fading channels, requiring no knowledge of the channel fading.

Hybrid Policy E_3

This policy is proposed for slow fading channels where small scale fading parameters estimation and their feedback to the decision making node is feasible.

$$E_3 = \{g_{sd}r_1^{-\alpha} \leq g_{sr}r_2^{-\alpha}, D \leq r_1\} \quad (2.15)$$

Note that this cooperation policy is still independent of the interference as in the pure geometric cooperation policy E_2 .

2.3.2 Cooperation Probabilities

In this part of the section we derive cooperation probabilities ρ_2 and ρ_3 for the policies E_2 and E_3 respectively. For the ideal policy E_1 , analytic evaluation of the cooperation probability is rather complicated because of the inter-dependency between the cooperation decision and consequential interference among different cells. Consider a random BS and its associated active UE. The distribution of the distance r_1 between the i^{th} UE and its associated BS can be shown to be Rayleigh distributed directly from the null probability of a two dimensional PPP distribution.

Due to the stationarity of the PPP, i.e., location of the origin doesn't change the distribution of points, and the independence of Φ_2 from BSs distribution we can assume that the location of the UE associated with the BS under study represents the origin point of Φ_2 . Then, each UE in Φ_1 chooses the closest UE in Φ_2 to assist it in relaying its message to the serving BS. Hence, similar to source-to-destination distance, the distribution of the source-to-relay distance r_2 between the i^{th} UE and its associated relaying UE can

be also shown to be Rayleigh distributed from the null probability of a two dimensional PPP. Therefore,

$$f_{r_1}(r_1) = 2\pi\lambda_1 r_1 e^{-\lambda_1 \pi r_1^2},$$

$$f_{r_2}(r_2) = 2\pi\lambda_2 r_2 e^{-\lambda_2 \pi r_2^2} \quad (2.16)$$

Theorem 2.1. *Cooperation Probabilities. The probability of deploying user-assisted relaying for a randomly located active user within a cell can be evaluated as follows:*

i. For policy E_2

$$\rho_2 = \int_{-\pi/2}^{-\pi/3} \frac{2\lambda_2 \cos^2 \psi_0}{\pi(\lambda_1 + 4\lambda_2 \cos^2 \psi_0)} d\psi_0 + \int_{\pi/3}^{\pi/2} \frac{2\lambda_2 \cos^2 \psi_0}{\pi(\lambda_1 + 4\lambda_2 \cos^2 \psi_0)} d\psi_0 + \frac{\lambda_2}{3(\lambda_1 + \lambda_2)} \quad (2.17)$$

ii. For policy E_3

$$\begin{aligned} \rho_3 = & \int_0^2 f_\beta(z) \int_{-\pi/2}^{-\cos^{-1}(z/2)} \frac{2\lambda_2 \cos^2 \psi_0}{\pi(\lambda_1 + 4\lambda_2 \cos^2 \psi_0)} d\psi_0 dz \\ & + \int_0^2 f_\beta(z) \int_{\cos^{-1}(z/2)}^{\pi/2} \frac{2\lambda_2 \cos^2 \psi_0}{\pi(\lambda_1 + 4\lambda_2 \cos^2 \psi_0)} d\psi_0 dz \\ & + \int_0^2 f_\beta(z) \frac{\lambda_2 z^2 \cos^{-1}(z/2)}{\pi(\lambda_1 + \lambda_2 z^2)} dz \\ & + \int_2^\infty f_\beta(z) \int_{-\pi/2}^{\pi/2} \frac{2\lambda_2 \cos^2 \psi_0}{\pi(\lambda_1 + 4\lambda_2 \cos^2 \psi_0)} d\psi_0 dz \end{aligned}$$

where $\beta = \left(\frac{g_{sr}}{g_{sd}}\right)^{1/\alpha}$ and $f_\beta(z)$ is pdf of β which can be shown to be

$$f_\beta(z) = \frac{\alpha z^{\alpha-1}}{(1+z^\alpha)^2} \quad (2.18)$$

Proof. i.

$$\begin{aligned} \rho_2 &= \mathbb{P}\{E_2\} \\ &= \mathbb{P}\{r_2 \leq r_1, r_1^2 + r_2^2 - 2r_1 r_2 \cos \psi_0 \leq r_1^2\} \\ &= \mathbb{P}\{r_2 \leq r_1, r_2 \leq 2r_1 \cos \psi_0\} \end{aligned}$$

when $|\psi_0| < \pi/3$, $r_1 < 2r_1 \cos \psi_0 \Rightarrow$ if $r_2 < r_1$, r_2 satisfies both inequalities. Accordingly, we define \mathcal{E}_1 and \mathcal{E}_2 as follows

$$\begin{aligned}\mathcal{E}_1 &= (2\pi)^2 \lambda_1 \lambda_2 \int_0^\infty \int_0^{2r_1 \cos \psi_0} r_1 r_2 e^{-\pi(\lambda_1 r_1^2 + \lambda_2 r_2^2)} dr_2 dr_1 \\ &= \frac{2\lambda_2 \cos^2 \psi_0}{\pi(\lambda_1 + 4\lambda_2 \cos^2 \psi_0)} \\ \mathcal{E}_2 &= (2\pi)^2 \lambda_1 \lambda_2 \int_0^\infty \int_0^{r_1} r_1 r_2 e^{-\pi(\lambda_1 r_1^2 + \lambda_2 r_2^2)} dr_2 dr_1 \\ &= \frac{\lambda_2}{2\pi(\lambda_1 + \lambda_2)}\end{aligned}$$

$$\begin{aligned}\text{Now, } \rho_2 &= \int_{-\pi/3}^{\pi/3} \mathcal{E}_2 d\psi_0 + 2 \int_{\pi/3}^{\pi/2} \mathcal{E}_1 d\psi_0 \\ &= \frac{\lambda_2}{3(\lambda_1 + \lambda_2)} + 2 \int_{\pi/3}^{\pi/2} \mathcal{E}_1 d\psi_0\end{aligned}$$

ii.

$$\rho_3 = \mathbb{P}\{E_3\} \quad (2.19)$$

$$= \mathbb{P}\{r_2 \leq \left(\frac{g_{sr}}{g_{sd}}\right)^{1/\alpha} r_1, r_1^2 + r_2^2 - 2r_1 r_2 \cos \psi_0 \leq r_1^2\} \quad (2.20)$$

$$= \mathbb{P}\{r_2 \leq \beta r_1, r_2 \leq 2r_1 \cos \psi_0\} \quad (2.21)$$

$$= \mathbb{P}\{r_2 \leq 2r_1 \cos \psi_0\} \quad \text{for } \beta > 2 \quad (2.22)$$

$$= \mathbb{P}\{r_2 \leq \beta r_1\} \quad \text{for } \beta < 2 \text{ and } |\psi_0| < \cos^{-1}(\beta/2) \quad (2.23)$$

$$= \mathbb{P}\{r_2 \leq 2r_1 \cos \psi_0\} \quad \text{for } \beta < 2 \text{ and } \cos^{-1}(\beta/2) < |\psi_0| < \pi/2 \quad (2.24)$$

$$\therefore \rho_3 = 2 \int_0^2 f_\beta(z) \int_{\cos^{-1}(z/2)}^{\pi/2} \mathcal{E}_1 d\psi_0 dz + \int_0^2 f_\beta(z) \int_{-\cos^{-1}(z/2)}^{\cos^{-1}(z/2)} \mathcal{E}_3 d\psi_0 dz \quad (2.25)$$

$$+ \int_2^\infty f_\beta(z) \int_{-\pi/2}^{\pi/2} \mathcal{E}_1 d\psi_0 dz \quad (2.26)$$

\mathcal{E}_1 is defined in part i. of the proof and $\mathcal{E}_3 = \frac{\lambda_2 z^2}{2\pi(\lambda_1 + \lambda_2 z^2)}$ which is nothing but \mathcal{E}_2 with $\lambda_2 = \lambda_2 z^2$. $f_\beta(z)$, the pdf of β , can be obtained as follows

$$\begin{aligned}
F_\beta(z) &= \mathbb{P}\left\{\left(\frac{x_1}{x_2}\right)^{1/\alpha} \leq z\right\} = \mathbb{P}\{x_1 \leq z^\alpha x_2\} \\
&= \int_0^\infty \int_0^{z^\alpha x_2} e^{-(x_1+x_2)} dx_1 dx_2 \quad \text{since } g_{sr}, g_{sd} \sim \text{Exp}(1) \\
&= 1 - \frac{1}{1+z^\alpha}, \quad z \in [0, \infty)
\end{aligned}$$

The pdf $f_\beta(z)$ is then obtained by differentiating $F_\beta(z)$:

$$f_\beta(z) = \frac{dF_\beta(z)}{dz} = \frac{\alpha z^{\alpha-1}}{(1+z^\alpha)^2} \quad z \in [0, \infty)$$

□

2.4 Interference Analysis

User-assisted relaying actually increases the amount of out- of-cell interference in the network as some idle users are now transmitting when relaying information of active users. It is therefore necessary to understand this out-of-cell interference power, particularly its distribution, in order to assess the overall impact of user-assisted relaying on system performance.

2.4.1 First Two Moments of Interference Power

Since it is difficult to describe the exact distribution of out-of-cell interference power, here we choose to model the interference power to the cell under study as a Gamma distribution by fitting the first two moments of the interference power analytically developed using stochastic geometry of the field of interferers outside that cell. The expressions for interference power can be developed from Eqs. 2.13.

$$\mathcal{Q}_{d,i}^b = \sum_{k \neq i} B_k \left| h_{sd}^{(k,i)} \right|^2 P_{s,k}^b + (1 - B_k) \left| h_{sd}^{(k,i)} \right|^2 P_{s,k} \quad (2.27)$$

$$\mathcal{Q}_{d,i}^m = \sum_{k \neq i} \left[B_k \left(\left| h_{sd}^{(k,i)} \right|^2 P_{s,k}^m + \left| h_{rd}^{(k,i)} \right|^2 P_{r,k}^m \right) \right] + (1 - B_k) \left| h_{sd}^{(k,i)} \right|^2 P_{s,k} \quad (2.28)$$

$$\mathcal{Q}_{r,i} = \sum_{k \neq i} B_k \left| h_{sr}^{(k,i)} \right|^2 P_{s,k}^b + (1 - B_k) \left| h_{sr}^{(k,i)} \right|^2 P_{s,k} \quad (2.29)$$

Theorem 2.2. *Interference Power Statistics For network-wide deployment of user-assisted relaying, the out-of-cell interference generated at the destination BS and the relaying UE have the following statistics:*

- i. *The first two moments, mean and variance, of interference power at the destination BS during the 1st and 2nd phase, respectively, are*

$$\mathbb{E}[\mathcal{Q}_{d,i}^b] = \frac{2\pi\lambda_1\zeta_1}{\alpha-2}R_c^{2-\alpha}, \quad \mathbb{E}[\mathcal{Q}_{d,i}^m] = \frac{2\pi\lambda_1\zeta_3}{\alpha-2}R_c^{2-\alpha} \quad (2.30)$$

$$\text{var}[\mathcal{Q}_{d,i}^b] = \frac{\pi\lambda_1\zeta_2}{\alpha-1}R_c^{2(1-\alpha)}, \quad \text{var}[\mathcal{Q}_{d,i}^m] = \frac{\pi\lambda_1\zeta_4}{\alpha-1}R_c^{2(1-\alpha)} \quad (2.31)$$

- ii. *The first two moments, mean and variance, of interference power at the idle UE associated as a relay with the i th active UE are*

$$\mathbb{E}[\mathcal{Q}_{r,i}] = \lambda_1\zeta_1 \int_0^{2\pi} \int_{R_c}^{\infty} (r^2 + D^2 - 2rD\cos\theta)^{\alpha/2} r dr d\theta \quad (2.32)$$

$$\text{var}[\mathcal{Q}_{r,i}] = \lambda_1\zeta_2 \int_0^{2\pi} \int_{R_c}^{\infty} (r^2 + D^2 - 2rD\cos\theta)^{\alpha/2} r dr d\theta \quad (2.33)$$

$$\text{where } \zeta_1 = \rho_1 P_{s,k}^b + (1 - \rho_1) P_{s,k} \quad (2.34)$$

$$\zeta_2 = 2[\rho_1 (P_{s,k}^b)^2 + (1 - \rho_1) P_{s,k}^2], \quad (2.35)$$

$$\zeta_3 = \rho_1 (P_{s,k}^m + P_{r,k}^m) + (1 - \rho_1) P_{s,k}, \quad (2.36)$$

$$\zeta_4 = 2[\rho_1 (P_{s,k}^m + P_{r,k}^m)^2 + (1 - \rho_1) P_{s,k}^2 - \rho_1 P_{s,k}^m P_{r,k}^m] \quad (2.37)$$

Proof.

$$\begin{aligned} \mathbb{E}[\mathcal{Q}_{d,i}^b] &= -\left. \frac{\partial \mathcal{L}_{\mathcal{Q}_{d,i}^b}(s)}{\partial s} \right|_{s=0}, \\ \text{var}[\mathcal{Q}_{d,i}^b] &= -\left. \frac{\partial^2 \mathcal{L}_{\mathcal{Q}_{d,i}^b}(s)}{\partial s^2} \right|_{s=0} - \left(\mathbb{E}[\mathcal{Q}_{d,i}^b] \right)^2 \end{aligned}$$

where $\mathcal{L}_{\mathcal{Q}_{d,i}^b}(s)$ is the Laplace transform of $\mathcal{Q}_{d,i}^b$ and $R_c = 1/2\sqrt{\lambda_1}$ is the cell radius. Means and variances of $\mathcal{Q}_{d,i}^m$, $\mathcal{Q}_{r,i}$ can be calculated similarly. \square

From the above results for interference power statistics, the interference power is directly proportional to both the active users density, λ_1 , and the transmission power levels represented by $\zeta_i, i \in [1 : 4]$ in Eqs. 2.34 - 2.37

2.4.2 Modelling Interference Power Distribution

A parameterized probability distribution, which includes a wide variety of curve shapes, is useful in the representation of data when the underlying model is unknown or difficult to obtain in closed form. A parameterized probability distribution is usually characterized by its flexibility, generality, and simplicity. Although distributions are not necessarily determined by their moments, the moments often provide useful information and are widely used in practice. It is shown that the Gamma distribution is a good approximation for the interference when the point under study is closer to the cell center, but fails to represent the actual interference distribution whenever the point under study is exactly at the cell edge. We use the same approach here and match a Gamma distribution to the first two moments of the interference power terms derived earlier in Theorem 2.2.

Gamma Distribution

The Gamma distribution is specified by a shape parameter k and a scale parameter θ . The pdf of a Gamma distributed RV $\gamma[k, \theta]$ is defined as

$$F_\gamma(q|k, \theta) = \frac{q^{k-1}e^{(-q/\theta)}}{\theta^k \Gamma(k)}$$

where the Gamma function $\Gamma(t)$ is defined as $\Gamma(t) = \int_0^\infty x^{t-1}e^{-x}dx$. The mean and variance of $\gamma[k, \theta]$ are $k\theta$ and $k\theta^2$ respectively.

Since we know mean and variance of interference powers, we can estimate the shape and scale parameters by using the formulae:

$$k_i = \frac{(\mathbb{E}[Q_i])^2}{\text{var}[Q_i]}, \theta_i = \frac{\text{var}[Q_i]}{\mathbb{E}[Q_i]} \quad (2.38)$$

2.5 Simulations and Results

2.5.1 Simulation Setting

All simulations were done on a square region of side length 200m. To generate active UEs in the region, the number of UEs is taken as a realization of poisson RV with parameter λ_1 and these number of UEs were uniformly distributed in the square region. The same is done to generate idle UEs but with parameter λ_2 . I discarded the UEs whose Voronoi region extends to infinity.

In theory, the base station of a UE is uniformly distributed in the Voronoi region of UE but there is no easy practical way to uniformly pick a point from a polygonal area. One method is to triangulate the polygonal Voronoi region, choose a triangle weighted by area, choose a point in that triangle. This is clearly quite complex to code so I've not implemented this method. The method I followed to generate BSs is - pick a number greater than or equal to the number of active UEs and distribute these number of BSs uniformly in the square region. Now go to each active UE and check if there are any BSs in its Voronoi region. If there are BSs, pick one of them and associate it with the UE and discard other BSs in the Voronoi region. Since BSs are distributed uniformly over the whole region, the result is as good as picking BSs uniformly in the Voronoi regions of UEs which is what we wanted but there is a catch. In the theoretical method, each UE with a finite Voronoi region is guaranteed to have a BS whereas in the way that I'm generating, some UEs might not have a BS even though their Voronoi region is of finite area. Further, the UEs without a BS are not included in rate or cooperation probability analysis which is logical since without an associated BS, the UEs cannot be considered active.

For all simulations, we assume that UEs are using maximum power to transmit without applying any power control method. The powers used during the two phases of transmission are as follows

- Source and relays use equal power $\Rightarrow P_{s,i} = P_{r,i}$
- Source use equal power during broadcast and multicast phases $\Rightarrow P_{s,i}^b = P_{s,i}^m$
- $P_{s,i}^{m1} = \beta_1 P_{s,i}^m$ and $P_{s,i}^{m2} = (1 - \beta_1) P_{s,i}^m$. Where β_1 is allocated optimally to maximize the transmission rate of the active user. To do this, rate is expressed as a function of β_1 and minimized negative rate using MATLAB tool *fminrnd*.

2.5.2 Results

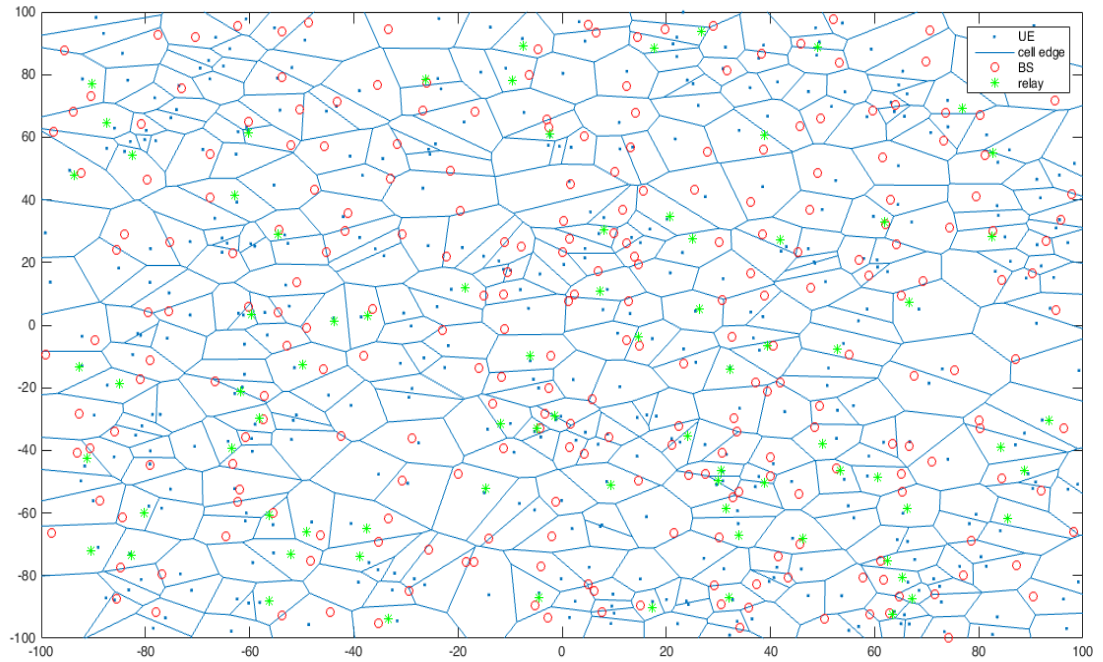
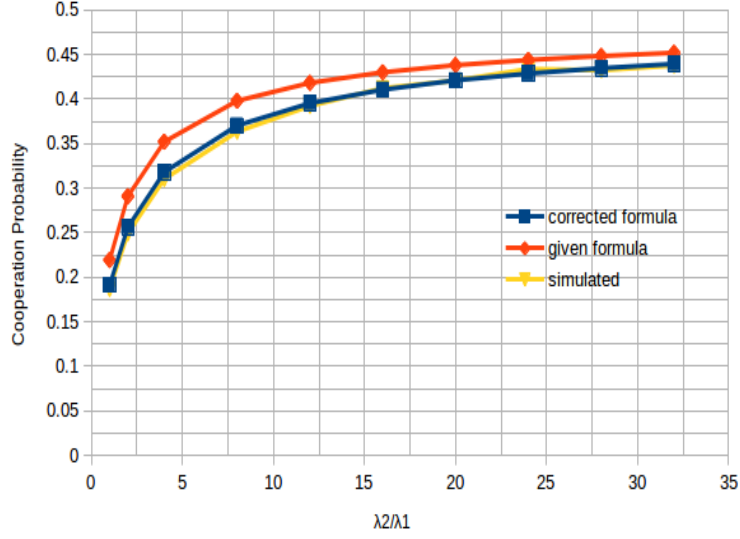
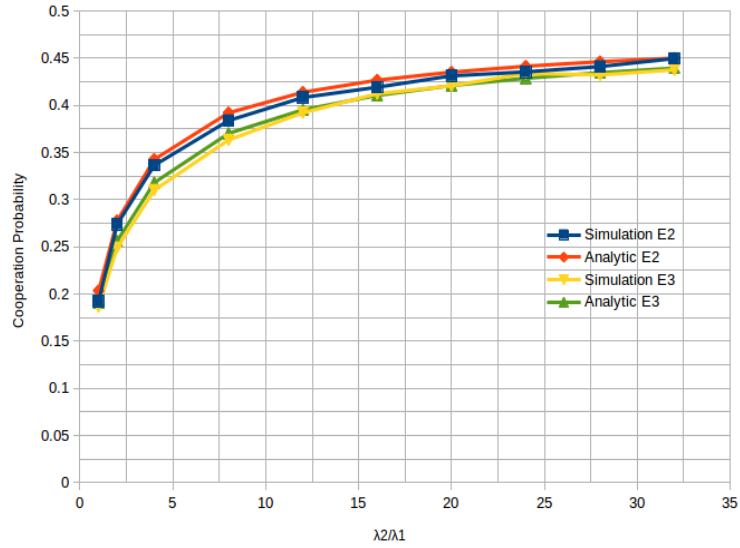


Figure 2.3: Network Layout

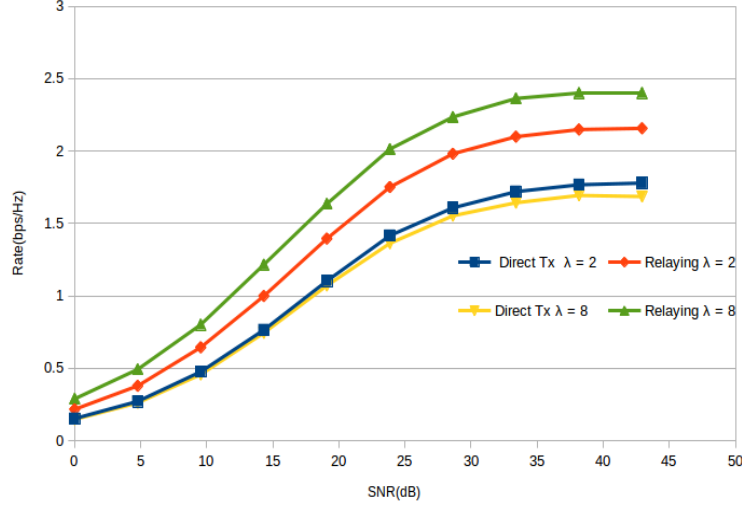
This is a sample network layout generated by using the method discussed in the previous subsection. We can see that some of the UEs are well within the range but have no BS. Only UEs with a BS are considered active. A fraction of active UEs have relays; these UEs use PDF relaying. Cooperation probability = number of active UEs with relays / total number of active UEs.

Figure 2.4: Corrected cooperation probability of E_3

In the published paper, the analytic result for cooperation probability of E_3 has an error. The correction being using \mathcal{E}_3 instead of \mathcal{E}_2 in eq. 2.26. The corrected analytic result matches the simulation result as can be seen in the above figure.

Figure 2.5: Cooperation probabilities of E_2 , E_3 versus user density ratio

From the above graph we can see that cooperation probability of both policies increases with user density ratio (λ_2/λ_1) and reach a maximum of 0.5 for very large user density ratio. Also, the analytic and simulations results closely match.

Figure 2.6: Average rate per user; $\lambda = \lambda_2/\lambda_1$

From the above figure, we can clearly see that average rate per user has increased when PDF relaying is deployed over the whole network. The rate also increases as user density ratio is increased but we can't be sure whether the rate keeps increasing with λ . It might happen that the rate decreases for very large user ratio density due to increase in interference.

2.6 Downlink Cooperation Policy

A cooperation policy for downlink can be defined along the same lines as we did in uplink case. Let P_b be the transmission power used by the base station and P_r be relay power. A simple distance based policy would be

$$\{P_b r_1^{-\alpha} > P_b R_0^{-\alpha}, P_r r_2^{-\alpha} > P_b R_0^{-\alpha}\}$$

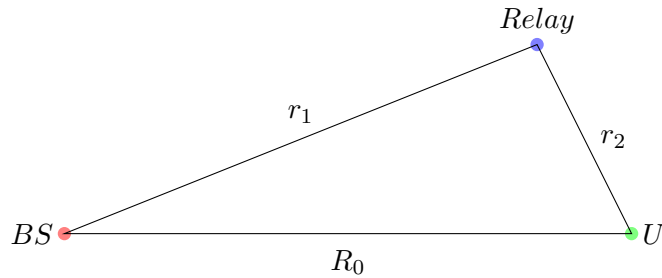


Figure 2.7: Distances for Downlink Cooperation

It can be rewritten as $\{r_1 < R_0, r_2 < R_2\}$ where $R_2 = cR_0, c = \left(\frac{P_r}{P_b}\right)^{\frac{1}{\alpha}}$ and r_1, r_2 are as defined in the figure 2.7. The two conditions in the policy ensure that both BS-relay and relay-user links are stronger than BS-user link. The policy dictates that the idle user should be located in the shaded part of figure 2.8 to be considered for relaying.

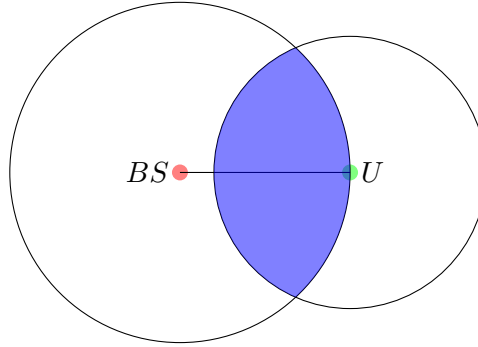


Figure 2.8: Feasible region

Although interference and cooperation probabilities are not analysed for downlink case, we will study relay mobility for this case. The reason being, downlink case presents a more general geometrical region of interest as compared to uplink where both circles are of same radius and some of the results derived can be directly adapted to uplink case by changing the corresponding parameters.

Chapter 3

Moving Relays

3.1 Mobility Model

In this section we describe two mobility models that are commonly used to study the effects of mobility in cellular networks. One is the classical random waypoint (RWP) model and the other is the RWP mobility model proposed in [1]. In classical RWP, the node selects the destination, called waypoint, uniformly from the whole domain and velocity is selected from a uniform distribution. The node then moves from current waypoint to next waypoint along a straight line at the velocity selected. The distance it travels in doing so is called *transition length* and the time *transition time*. We will not use the classical RWP model as the transition lengths in this model are of the order of size of domain which is not the case in mobility of relays in cellular networks. Also, as noted in [1], Rayleigh RWP compares well with synthetic Levy Walk, which is constructed from real mobility trajectories, in terms of CDFs of transition length and direction switch rates than classical RWP model.

3.1.1 Rayleigh RWP Model

We define mobility more formally and introduce the model proposed in [1]. The n th transition of a node can be denoted by the parameters set $(\mathbf{X}_{n-1}, \mathbf{X}_n, V_n, S_n)$. \mathbf{X}_{n-1} denotes the starting waypoint and \mathbf{X}_n denotes the destination. In addition to the transition time which can be obtained from velocity V_n , pause time or thinking time (S_n) at destination can also be included in the description of mobility. Different mobility models can be distinguished by the distribution of transition length ($L_n = \|\mathbf{X}_{n-1} - \mathbf{X}_n\|$) and the

distribution of angle made by the vector $\mathbf{X}_n - \mathbf{X}_{n-1}$ w.r.t x-axis. In Rayleigh RWP, the angle is chosen uniformly from $[0, 2\pi]$ and the transition length is rayleigh distributed with parameter λ .

$$P(L > l) = \exp(-\lambda \pi l^2), l \geq 0 \quad (3.1)$$

We set $V_n \equiv v$ and S_n to 0. What the above selection of distributions means is that when the node is at waypoint \mathbf{X}_{n-1} , a homogenous Poisson Point Process ϕ of intensity λ is generated and the nearest point in the set is chosen as the next waypoint \mathbf{X}_n . i.e., $\mathbf{X}_n = \arg \min_{x \in \phi} \|x - \mathbf{X}_{n-1}\|$. This can be proved from the null distribution of PPP. This gives better insight in to the role of parameter λ . Larger λ implies that the points are denser in generated PPP which in turn means the transition length is shorter. Figure 3.1 shows sample traces of rayleigh RWP for different λ . Please note that the figures are scaled differently.

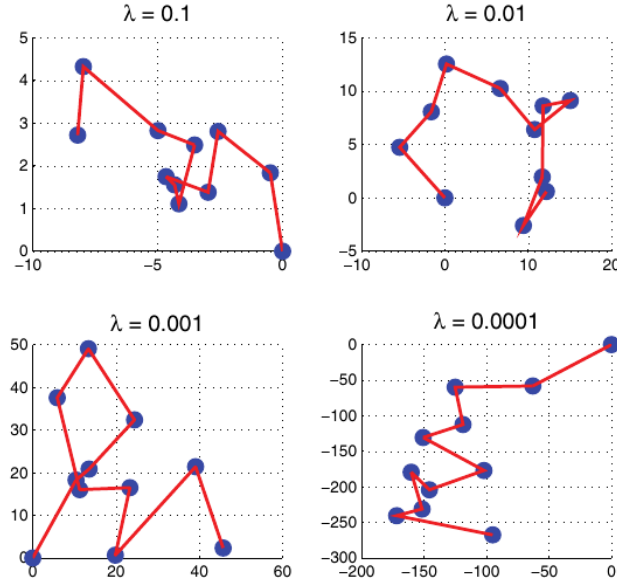


Figure 3.1: The transition lengths are statistically shorter with larger mobility parameter λ , and vice versa.¹

The mean transition length and time are as follows:

$$E[L] = \frac{1}{2\sqrt{\lambda}} \quad (3.2)$$

$$E[T] = \frac{1}{2v\sqrt{\lambda}} \quad (3.3)$$

¹Image Source: [1] Xingqin Lin et al.

both of which can be easily derived from distribution of L .

3.2 Mean Sojourn Time

Sojourn time is the amount of time a node resides in the region of interest. Calculating the mean sojourn time is challenging primarily because it involves finding node distribution during each transition. An expression for mean sojourn time of a cell user during one movement period starting from origin in a hexagonal cell was given in [1]. We have to note that a moving node usually makes more than one transition before it leaves the region. Also, starting from origin implies the node co-exists with BS at $t=0$ which is not representative of the distribution of relays/users. Even if we allow these two assumptions, the problem is still difficult to solve in this approach as the region has no definite shape like a polygon and finding integration limits is tedious. If we know the expected number of transitions $E[N]$ a node makes before moving out of the region, then sojourn time can be given by

$$S_T = (E[N] - 1)E[T] + E[T_{last}]$$

where T_{last} is the time spent inside the region during the last transition. Since it is difficult to characterize T_{last} , we approximate S_T to $(E[N] - 1)E[T]$. The general form of the expression for $E[N]$ is

$$E(N) = \sum_{k=1}^{\infty} k Pr(r, \theta, k)$$

where

$$Pr(r, \theta, k) = \int_{S-A} \int_A \int \dots \int_A f_{X_1/X_0}(x_1/x_0) f_{X_2/X_1}(x_2/x_1) \dots f_{X_{k+1}/X_k}(x_{k+1}/x_k) dA_1 dA_2 \dots dA_{k+1}$$

is the probability that the node exits the region during $k+1$ th transition. $f_{X_n/X_{n-1}}(x_n/x_{n-1})$ is the probability density of the destination X_n given that the node's current position is X_{n-1} . $X_0 = (r, \theta)$ is where the node starts the movement at $t=0$, A is the feasibility region and S is the entire plane. As a first step towards finding $E[N]$, let us find the probability with which a node at (r, θ) leaves the region in one transition.

3.3 Probability of leaving in one transition

To know whether or not the node is outside the region, we have to find the boundaries it has to cross in each direction. To do this we use plane geometry and trigonometry to find necessary distances and angles.

3.3.1 Boundaries of the region

Consider the figure 3.2. The node starts at B and let C be the destination during first

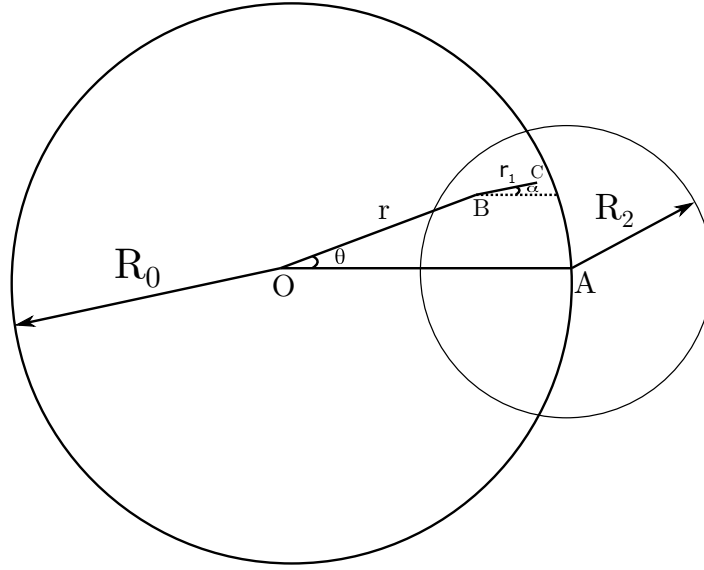


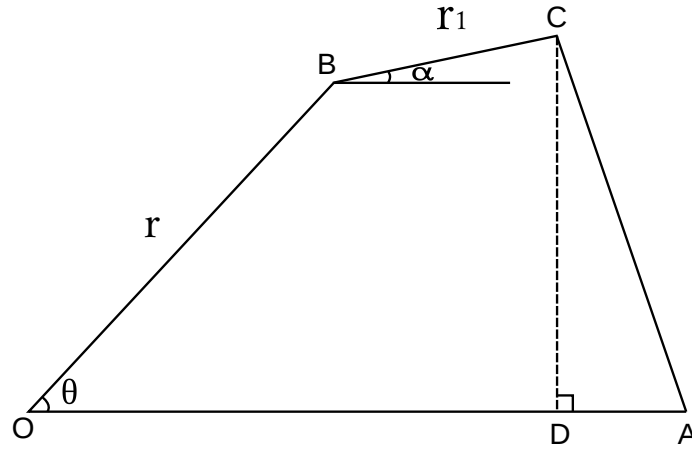
Figure 3.2: Initial Position is (r, θ)

transition. α, r_1 are chosen according to the mobility model described in the previous section. Whether or not C is outside the region depends on its distance from the circles' centers O and C . OC can be found using cosine rule: $OC^2 = OB^2 + BC^2 - 2 \cdot OB \cdot BC \cdot \cos(\angle CBO)$. $\angle CBO = \pi - \theta + \alpha$ (see figure 3.3).

Therefore,

$$OC^2 = r^2 + r_1^2 + 2rr_1 \cos(\theta - \alpha) \quad (3.4)$$

To find AC , drop a perpendicular from C to the line OA and let the intersection point

Figure 3.3: Initial Position is (r, θ)

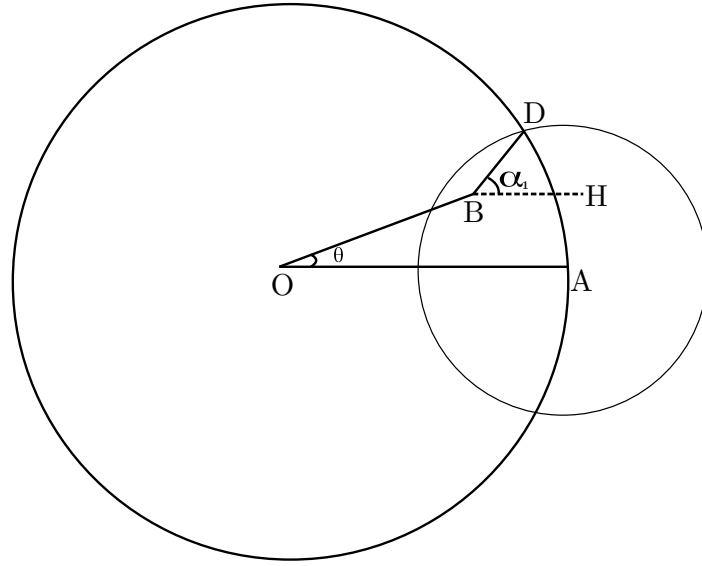
be D as shown in figure 3.3. Consider $\triangle CDA$,

$$\begin{aligned}
 CD &= OB \sin \theta + BC \sin \alpha \\
 &= r \sin \theta + r_1 \sin \alpha \\
 DA &= OA - OB \cos \theta - BC \cos \alpha \\
 &= R_0 - r \cos \theta - r_1 \cos \alpha
 \end{aligned}$$

Since $\angle CDA = \pi/2$, $AC^2 = CD^2 + DA^2$. AC can therefore be given by

$$AC^2 = (r \sin \theta + r_1 \sin \alpha)^2 + (R_0 - r \cos \theta - r_1 \cos \alpha)^2 \quad (3.5)$$

To find which circle the node crosses first, we also need the angle made by the circle intersections at B . Let α_1 and α_2 be as shown in figures 3.4 and 3.6 where BH is a horizontal line.

Figure 3.4: α_1

In figure 3.4, join OD and drop a perpendicular from D to meet the extension of the OB at E . To avoid clutter, let us remove the circles and form figure 3.5. Consider

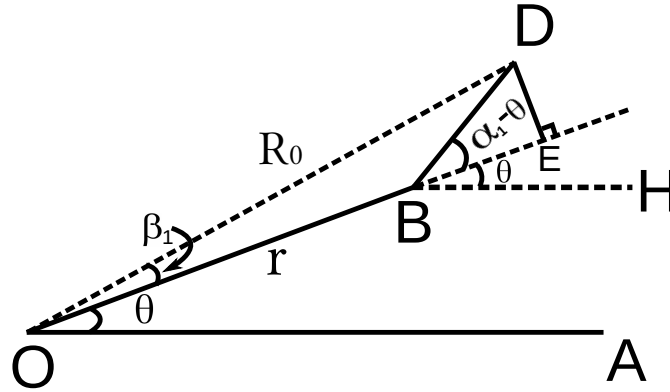


Figure 3.5: Previous fig. without circles

$\triangle DOA$,

$$AD^2 = OD^2 + OA^2 - 2 \cdot OD \cdot OA \cdot \cos(\beta_1 + \theta)$$

$$R_2^2 = R_0^2 + R_0^2 - 2R_0^2 \cos(\beta_1 + \theta)$$

$$\beta_1 = \cos^{-1} \left(1 - \frac{R_2^2}{2R_0^2} \right) - \theta \quad (3.6)$$

Using β_1 we can find α_1

$$\begin{aligned}\tan(\alpha_1 - \theta) &= \frac{DE}{BE} \\ &= \frac{DE}{OE - OB} \\ &= \frac{R_0 \sin \beta_1}{R_0 \cos \beta_1 - r} \\ \alpha_1 &= \theta + \tan^{-1} \left(\frac{R_0 \sin \beta_1}{R_0 \cos \beta_1 - r} \right)\end{aligned}$$

α_2 and β_2 are defined in figures 3.6 and 3.7. $\beta_2 = \beta_1 + \theta$ by symmetry. Using expression

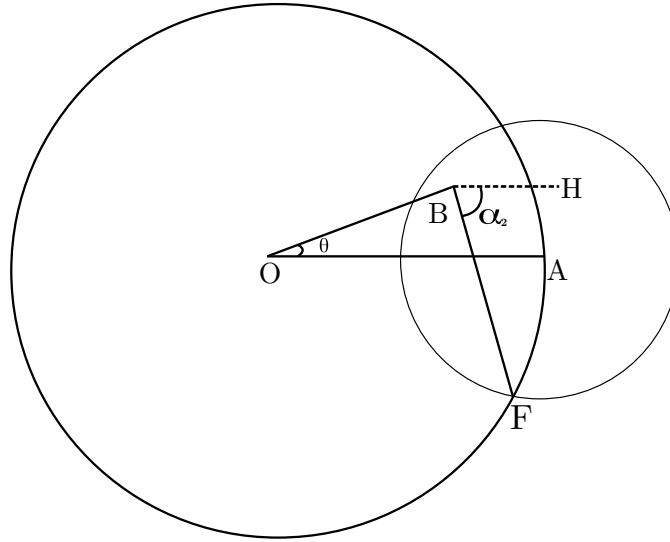
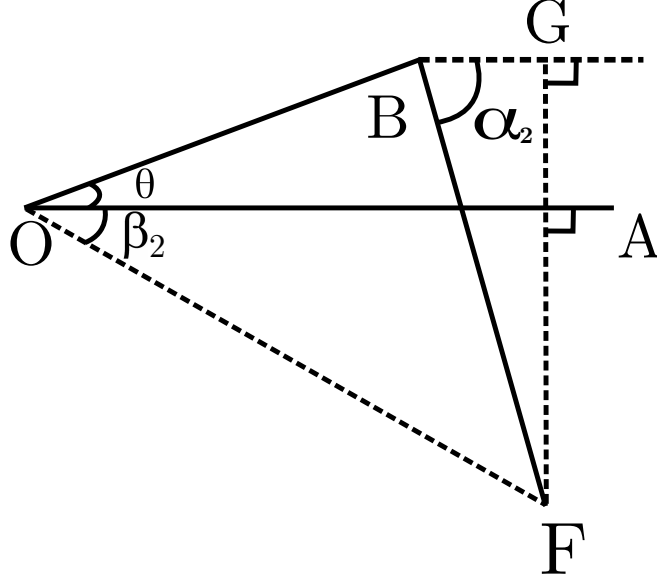


Figure 3.6: α_2

3.6 for β_1 , we get

$$\beta_2 = \cos^{-1} \left(1 - \frac{R_2^2}{2R_0^2} \right) \quad (3.7)$$

To find α_2 , consider $\triangle BGF$ in figure 3.7

Figure 3.7: α_2 without circles

$$\begin{aligned}
 \tan \alpha_2 &= \frac{FG}{GB} \\
 &= \frac{FA + AG}{GB} \\
 &= \frac{R_0 \sin \beta_2 + r \sin \theta}{R_0 \cos \beta_2 - r \cos \theta} \\
 \Rightarrow \alpha_2 &= \tan^{-1} \left(\frac{R_0 \sin \beta_2 + r \sin \theta}{R_0 \cos \beta_2 - r \cos \theta} \right)
 \end{aligned}$$

3.3.2 Probability

When $-\alpha_2 < \alpha < \alpha_1$, C is outside the region if $OC^2 > R_0^2$ (see 3.3) and for other values of α , the node leaves the region if $AC^2 > R_2^2$. The probability of node leaving the region in one transition, let us call it $\rho(r, \theta)$, is given by

$$\rho(r, \theta) = Pr(-\alpha_2 < \alpha < \alpha_1, OC^2 > R_0^2) + Pr(\alpha_1 < \alpha < 2\pi - \alpha_2, AC^2 > R_2^2) \quad (3.8)$$

Let us rewrite the above in terms of r_1 whose distribution we know. $AC^2 > R_2^2 \Rightarrow$

$$\begin{aligned}
& (r \sin \theta + r_1 \sin \alpha)^2 + (R_0 - r \cos \theta - r_1 \cos \alpha)^2 > R_2^2 \\
& r_1^2 \sin^2 \alpha + r^2 \sin^2 \theta + 2rr_1 \sin \theta \sin \alpha + \\
& (R_0 - r \cos \theta)^2 + r_1^2 \cos^2 \alpha - 2(R_0 - r \cos \theta)r_1 \cos \alpha - R_2^2 > 0 \\
& r_1^2 + 2r_1(r \sin \alpha \sin \theta - (R_0 - r \cos \theta) \cos \alpha) + r^2 \sin^2 \theta + (R_0 - r \cos \theta)^2 - R_2^2 > 0 \\
& r_1^2 + 2(r \cos(\theta - \alpha) - R_0 \cos \alpha)r_1 + r^2 \sin^2 \theta + (R_0 - r \cos \theta)^2 - R_2^2 > 0
\end{aligned}$$

The above inequality gives two feasible intervals for r_1 one of which is spurious since $r_1 > 0$ and the other is

$$r_1 > (R_0 \cos \alpha - r \cos(\theta - \alpha)) + \sqrt{(R_0 \cos \alpha - r \cos(\theta - \alpha))^2 + R_2^2 - r^2 \sin^2 \theta - (R_0 - r \cos \theta)^2} \quad (3.9)$$

Similar calculations as above will reduce $OC^2 > R_0^2$ to

$$r_1 > -r \cos(\theta - \alpha) + \sqrt{R_0^2 - r^2 \sin^2(\theta - \alpha)} \quad (3.10)$$

Let us denote the R.H.S of the above two inequalities by r_{12} and r_{11} respectively. Substituting 3.9 and 3.10 in 3.8, we get

$$\begin{aligned}
\rho(r, \theta) &= Pr(-\alpha_2 < \alpha < \alpha_1, r_1 > r_{11}) + Pr(\alpha_1 < \alpha < 2\pi - \alpha_2, r_1 > r_{12}) \\
&= \int_{-\alpha_2}^{\alpha_1} \int_{r_{11}}^{\infty} f_{r_1, \alpha}(r_1, \alpha) dr_1 d\alpha + \int_{\alpha_1}^{2\pi - \alpha_2} \int_{r_{12}}^{\infty} f_{r_1, \alpha}(r_1, \alpha) dr_1 d\alpha
\end{aligned}$$

This is a general expression that can be used for any mobility model. In case of RWP, r_1 and α are chosen independently. Therefore, $f_{r_1, \alpha}(r_1, \alpha) = f_{r_1}(r_1)f_{\alpha}(\alpha)$

$$\begin{aligned}
\rho(r, \theta) &= \int_{-\alpha_2}^{\alpha_1} f_{\alpha}(\alpha) \int_{r_{11}}^{\infty} f_{r_1}(r_1) dr_1 d\alpha + \int_{\alpha_1}^{2\pi - \alpha_2} f_{\alpha}(\alpha) \int_{r_{12}}^{\infty} f_{r_1}(r_1) dr_1 d\alpha \\
&= \int_{-\alpha_2}^{\alpha_1} \frac{1}{2\pi} e^{-\lambda \pi r_{11}^2} d\alpha + \int_{\alpha_1}^{2\pi - \alpha_2} \frac{1}{2\pi} e^{-\lambda \pi r_{12}^2} d\alpha
\end{aligned}$$

Putting it all together at one place for ease of reference, this is what we have about the node's first transition.

The probability with which a node at (r, θ) moves out of the region of interest during the next transition is

$$\rho(r, \theta) = \int_{-\alpha_2}^{\alpha_1} \frac{1}{2\pi} e^{-\lambda\pi r_{11}^2} d\alpha + \int_{\alpha_1}^{2\pi-\alpha_2} \frac{1}{2\pi} e^{-\lambda\pi r_{12}^2} d\alpha \quad (3.11)$$

Where

$$r_{11} = -r \cos(\theta - \alpha) + \sqrt{R_0^2 - r^2 \sin^2(\theta - \alpha)}$$

$$r_{12} = R_0 \cos \alpha - r \cos(\theta - \alpha) + \sqrt{[R_0 \cos \alpha - r \cos(\theta - \alpha)]^2 - r^2 \sin^2 \theta - [R_0 - r \cos \theta]^2 + R_2^2}$$

$$\beta_1 = \cos^{-1} \left(1 - \frac{R_2^2}{2R_0^2} \right) - \theta$$

$$\beta_2 = \cos^{-1} \left(1 - \frac{R_2^2}{2R_0^2} \right)$$

$$\alpha_1 = \theta + \tan^{-1} \left(\frac{R_0 \sin \beta_1}{R_0 \cos \beta_1 - r} \right)$$

$$\alpha_2 = \tan^{-1} \left(\frac{r \sin \theta + R_0 \sin \beta_2}{R_0 \cos \beta_2 - r \cos \theta} \right)$$

3.4 Expected number of transitions

Let us make a gross approximation and use the same probability of leaving for all way-points in the path. Then the average number of steps a node starting at (r, θ) takes to

leave the region is given by

$$\begin{aligned} E[N] &= \sum_{k=1}^{\infty} k(1 - \rho(r, \theta))^{k-1} \rho(r, \theta) \\ &= \frac{1}{\rho(r, \theta)} \end{aligned}$$

Although the above approximation is not valid, this approach is useful when deriving upper and lower bounds on $E[N]$ as we shall see in the next chapter.

Chapter 4

Mobility Markov Chain

The transitions in this mobility model have Markovian property in the sense that the next waypoint depends entirely on the current position.

$$f_{X_n/X_{n-1}, X_{n-2}, \dots, X_0}(x_n/x_{n-1}, x_{n-2}, \dots, x_0) = f_{X_n/X_{n-1}}(x_n/x_{n-1})$$

Where X_{n-1} is the current waypoint and X_n is the next waypoint.

The idea is to discretize the state space of this Markov chain and model the motion as an Absorbing Markov Chain in which the node transitions among the non-absorbing states present inside the region before finally moving to the absorbing state. Let the whole space be represented by $n + 1$ states of which n states lie inside the region of interest and the $n + 1$ th state represents the space outside the region. The transition probabilities among first n states depend on the distances between the nodes and the transition probabilities from these n states to the absorbing state is $\rho(r_i, \theta_i)$ where (r_i, θ_i) is the position of the i th state. We can then use the expressions given in [3] to find expected value and variance of the number of transitions a node makes before getting absorbed in the $(n + 1)$ th state. The transition probability matrix of this Markov Chain is

$$P = \begin{pmatrix} Q & R \\ \mathbf{0} & 1 \end{pmatrix}$$

Where $Q_{n \times n}$ is the transition probability matrix of n non-absorbing states and $R_{n \times 1}$ contains the probabilities of moving out in one step from each of those n states. $\mathbf{t}_{n \times 1}$,

the vector which contains expected number of transitions, is given by

$$\mathbf{t} = A\mathbf{1}$$

and the variance vector V is given by

$$V = (2A - I)\mathbf{t} - \mathbf{t}_{sq}$$

where $A = \sum_{k=0}^{\infty} Q^k = (I - Q)^{-1}$ is the fundamental matrix.

It remains to be seen how well this model works.

Chapter 5

Simulations and Results

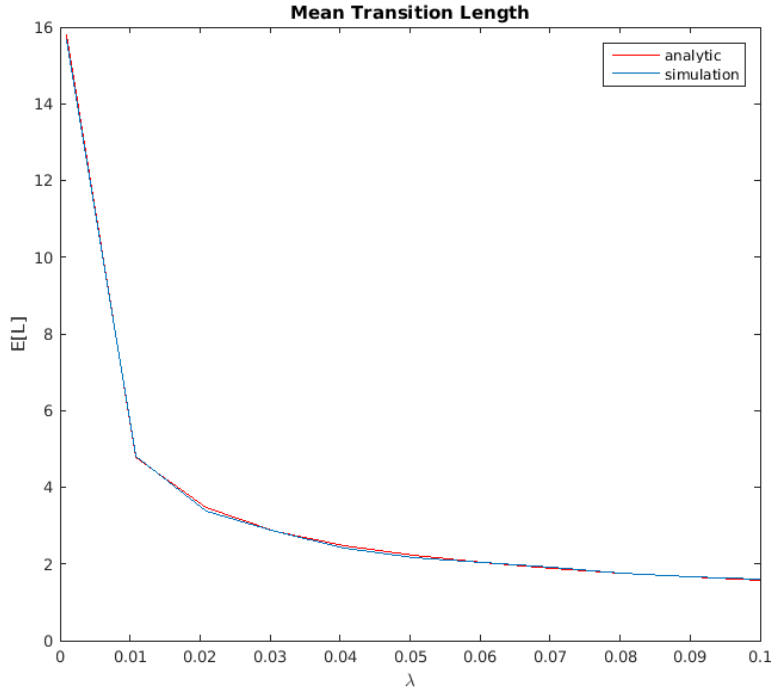
For all simulations, a 1000x1000 square is used to represent the whole 2-D plane. This size is good enough in the sense that using a larger square led to longer runtimes with little to no effect on the results. In the mobility model we used, transition length is Rayleigh distributed. To draw a length from Rayleigh distribution, the following method is used:

1. Draw a number N from Poisson distribution with density λA where A is the area of the square.
2. Distribute these N points uniformly on the square
3. Of these N points, choose the point that is closest to the point under consideration.

As discussed in [4], this leads to Rayleigh distribution of transition length and can be proved easily using null probability of a Poisson Point Process.

5.1 $E[L]$

To test if the above mentioned method introduces any artefacts, let us see how simulated $E[L]$ fares with the formula $E[L] = \frac{1}{2\sqrt{\lambda}}$. Simulated expected length is calculated by averaging transition lengths of 100 traces in each of which the node makes 1000 transitions. As seen in the graph 5.1, the simulated value closely follows the analytical formula.

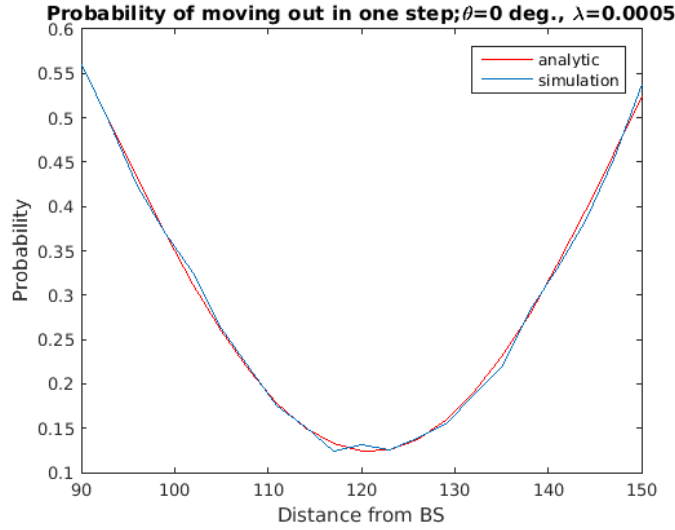
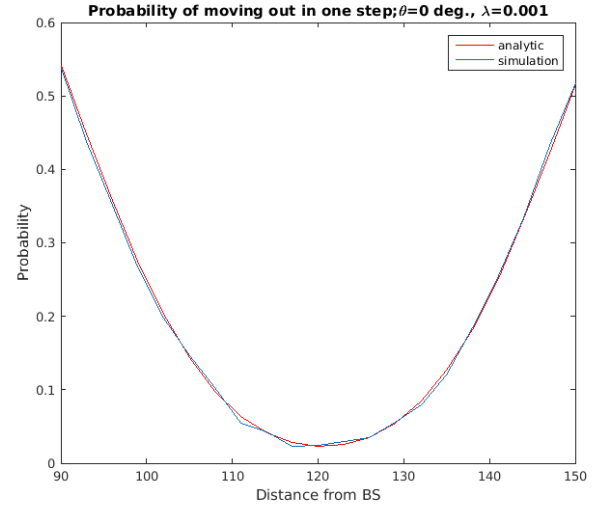
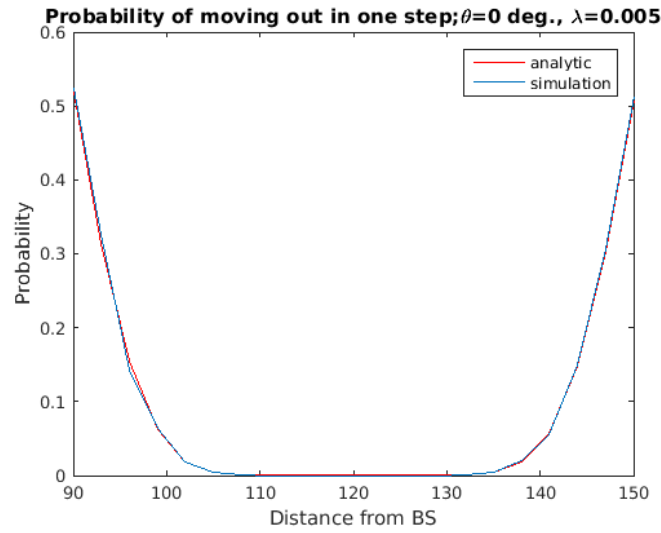
Figure 5.1: Mean transition length vs. λ

5.2 $\rho(r, \theta)$

In this section we look at how the probability $\rho(r, \theta)$ of moving out in one step varies in the region i.e., for different r and θ and with the mobility parameter λ .

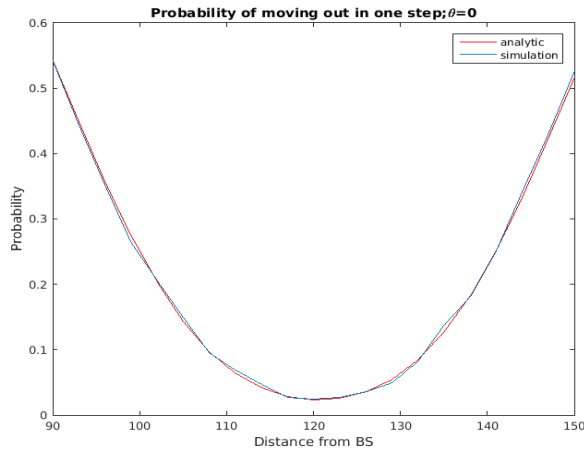
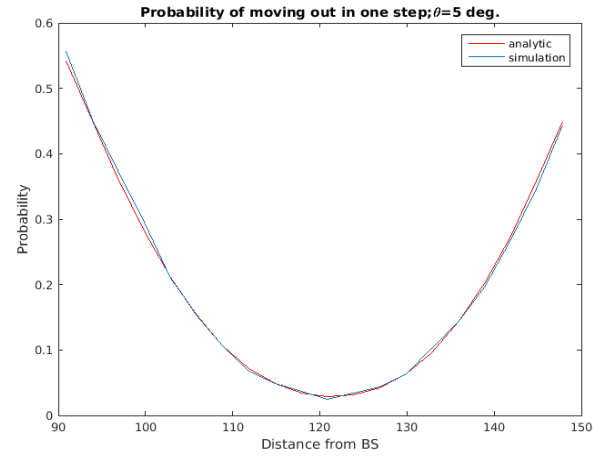
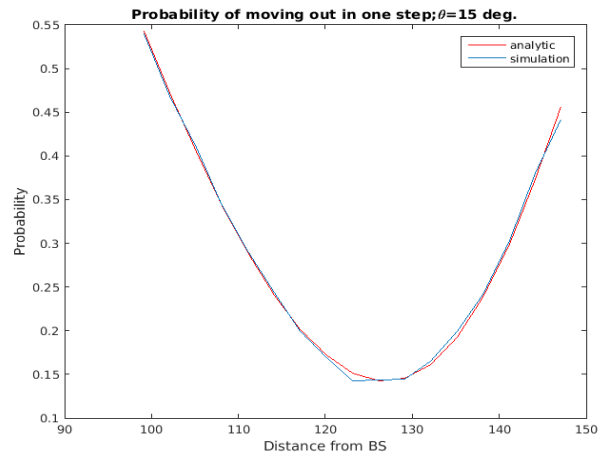
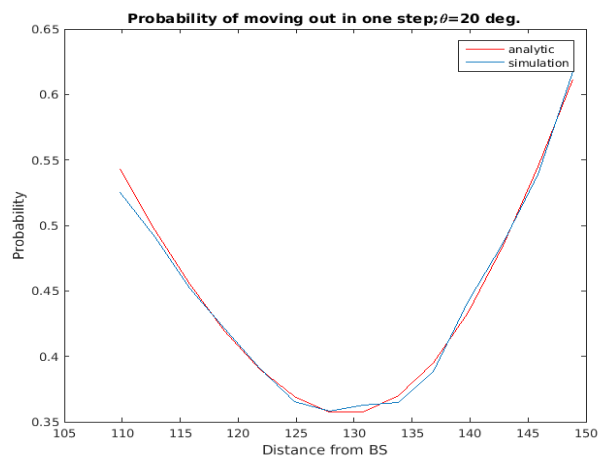
5.2.1 $\rho(r, \theta)$ vs. λ

The plots in figure 5.2 are for points inside the region and along the line joining centers of circles. At each iteration the node is placed at $(r, 0)$ and a PPP(λ) is generated. Probability is calculated by taking expected value of the indicator random variable which takes value 1 if the nearest point in PPP is outside the region and 0 if it is inside the region. What we can observe in figure 5.2 is that the probability for the points well within the region decreases as λ is increased. For points near the boundary of the region, the probability doesn't change significantly. This is in line with what is expected. For points well inside the region, $E[L]$ primarily decides whether or not they leave the region and for points closer to the boundary, the probability depends on the choice of angle α .

(a) $\lambda = 0.0005$ (b) $\lambda = 0.001$ (c) $\lambda = 0.005$ Figure 5.2: $\rho(r, 0)$ vs. λ

5.2.2 $\rho(r, \theta)$ for different θ

Figure 5.3 shows how $\rho(r, \theta)$ along the radius changes with θ . We can see that it increases with θ for points inside the region and doesn't change significantly for points at the edges. We can see that the maximum can occur at both edges.

(a) $\theta = 0^\circ$ (b) $\theta = 5^\circ$ (c) $\theta = 15^\circ$ (d) $\theta = 20^\circ$ Figure 5.3: $\rho(r, \theta)$ at different angles

5.3 $E[N]$

Figure 5.4 shows the expected number of steps in which a node leaves the region. The plots are for points along the radius at angles $\theta = 10^\circ$ and $\theta = 15^\circ$. We can see that the analytical formula agrees better for narrower regions. As discussed in Chapter 4, this can be improved by modelling the motion of a node as an absorbing Markov Chain and discretizing the state space.

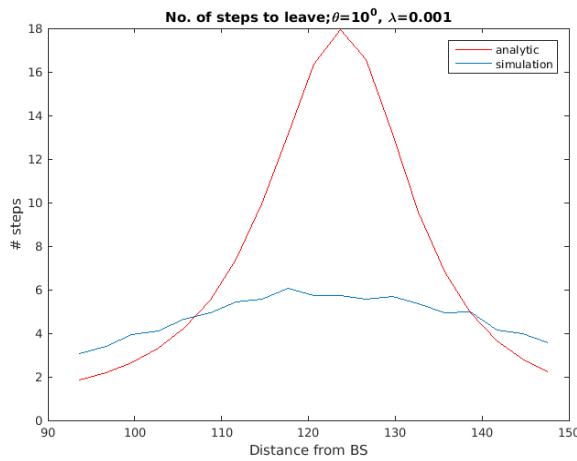
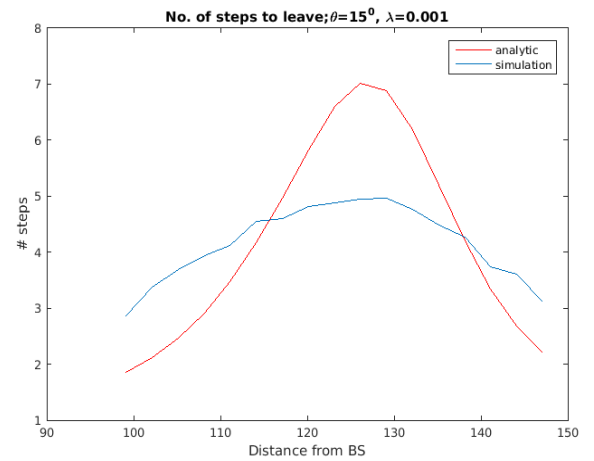
(a) $\theta = 10^\circ$ (b) $\theta = 15^\circ$

Figure 5.4: Expected number of transitions

Chapter 6

Conclusion and Further Work

6.1 Conclusion

Based on the results obtained we conclude the following:

- Based on the work of H. Elkotby, we verified that there is throughput gain when user-assisted relaying is deployed in cellular network despite the increase in interference.
- We proposed a downlink cooperation policy following the same logical reasoning that was used for uplink policies.
- We briefly discussed the importance of relay mobility as a decision parameter in relay selection.
- We gave a general expression for the probability that a node leaves the feasible region that can be used for any mobility model.
- The probability of leaving the region is maximum for points on the boundary. The maximum shifts to right side border for points closer to intersection of circles.
- The expected number of transitions can be better approximated by discretizing the region as states in a Markov Chain.

6.2 Further Work

The following can be looked at in the future.

-
- Using the idea presented in chapter 4 to obtain lower and upper bounds on the expected number of steps if not to find the the value itself to a close apprximation.
 - Through out the work we took R_0 , the distance between base station and user, to be constant and did not assume the distribution of inital position of the relay. The distributions of R_0 and initial position can be incorporated to find the effect of mobility on the whole network.
 - To include sojourn time as one of the deciding parameters in relay selection.
 - To apply the general methodology used in this work for other mobility models.

Bibliography

- [1] X. Lin, R. K. Ganti, P. J. Fleming, and J. G. Andrews, “Towards understanding the fundamentals of mobility in cellular networks,” *IEEE Transactions on Wireless Communications*, vol. 12, 2013.
- [2] H. Elkotby and M. Vu, “Interference and throughput analysis of uplink user-assisted relaying in cellular networks,” *PIMRC*, 2014.
- [3] Wikipedia, “Absorbing markov chain — wikipedia, the free encyclopedia,” 2016. [Online; accessed 17-June-2016].
- [4] R. K. Ganti, “Stochastic geometry and wireless networks.” SPCOM, July 2012.